Electronic effects in the formation of apparently noisy scanning tunneling microscopy images of Sr on Si(111)-7×7

R. Zhachuk,[1,2] B. Olshanetsky,[1] J. Coutinho,[3] and S. Pereira[2]
[1]*Institute of Semiconductor Physics, Pr. Lavrentyeva 13, Novosibirsk 630090, Russia*
[2]*CICECO, University of Aveiro, Campus Santiago, 3810-193 Aveiro, Portugal*
[3]*I3N, University of Aveiro, Campus Santiago, 3810-193 Aveiro, Portugal*
(Received 4 February 2010; revised manuscript received 26 March 2010; published 16 April 2010)

The potential-energy surface (PES) for Sr adsorption on Si(111)-7×7 is calculated within density-functional theory. The main diffusion paths and corresponding energy barriers are determined for a Sr atom on reconstructed Si(111) surface. Comparison of simulated and experimental scanning tunneling microscopy (STM) images of apparently noisy patches in halves of 7×7 unit cells shows good agreement with respect to bias and polarity dependence. It was found that Sr thermal motion alone cannot account for the apparently noisy STM image patches. The origin of the peculiar intensity distribution in those images is due to charge transfer from the Sr atom to Si adatoms in the 7×7 reconstruction. Thus, electronic effects complement the picture and enable to understand the observations. With this knowledge in hand, the contradiction between experimental apparently noisy STM image patches and calculated PES for other adsorbates is readily explained.

DOI: 10.1103/PhysRevB.81.165424 PACS number(s): 68.35.Fx, 68.43.Bc, 71.15.Mb, 71.15.Pd

I. INTRODUCTION

Besides the fundamental scientific interest, Sr adsorption on silicon surfaces has attracted considerable attention due to the possibility of growing $SrTiO_3$ high-k dielectric layers on top of silicon.[1] This is one of the main contenders to replace SiO_2 in sub-32 nm gate length complementary metal oxide semiconductor technology. Sr adsorption on Si(111) surface has been recently investigated by scanning tunneling microscopy (STM).[2,3] These experiments revealed highly mobile Sr adatoms at room temperature (RT) trapped within the 7×7 half-unit cell (HUC) boundaries. Such motion originates fuzzy or apparently noisy patches in the STM images that have been found earlier for other adsorbates such as Si, Pb, Tl, Sn, Ag, and Y.[4–6]

Several theoretical studies have been dedicated to adatom adsorption and diffusion on Si(111)-7×7. In the pioneering work by Cho and Kaxiras, the authors used a 4×4 supercell to mimic the local 2×2 arrangement of adatoms in the Si(111)-7×7 reconstruction.[7] They found that the most stable adsorption sites or basins of attraction for K, Mg, Ga, and Ge atoms are located around Si rest atoms in 7×7 HUCs, while the surface dangling-bond sites show energy maxima. These results are different from the adsorption of the H atom on the Si(111)-7×7 surface. Here, the Si radical sites are found to be the most stable positions because the hydrogen atom has one coordination number.[8] *Ab initio* studies of Pb and Si adsorption using complete 7×7 supercells showed that sites located in a basin of attraction and close to the HUC center are slightly more stable than sites located close to corner holes.[9,10] Using a direct mapping of the potential-energy surface (PES) for a Si adatom on a complete 7×7 reconstruction, the authors identified an additional basin around the HUC center and determined diffusion paths to neighboring HUC.[10]

Although adatom adsorption and diffusion on the Si(111)-7×7 surface have been studied both experimentally and theoretically earlier, there was no estimation of the average speed of the captured atom observed in STM as an apparently noisy patch. Moreover, the change of the surface electronic structure due to foreign atom adsorption and its impact on resulting STM images was not analyzed previously. This led to an incorrect interpretation of the intensity distribution in some experimental STM images as demonstrated below.

Here we present the results of our STM study complemented with density-functional theoretical (DFT) calculations of the adsorption and diffusion of a single Sr adatom on Si(111)-7×7. From the self-consistent charge density, we simulate STM imagery of the Sr atom trapped at 7×7 HUC and compare them to the experimental images of apparently noisy patches obtained at various voltages. We use the resulting calculated stable adsorption sites to generate simulated STM images of Sr atoms trapped within the 7×7 HUC so that a more accurate interpretation of fine features of the apparently noisy patches can be achieved. It is demonstrated that STM images of apparently noisy patches cannot be understood properly without taking into account the charge transfer from the Sr atom to Si adatoms at the 7×7 reconstruction.

II. EXPERIMENTAL AND COMPUTATIONAL DETAILS

Experiments were performed in ultrahigh vacuum system with a base pressure of about 9×10^{-11} Torr equipped with STM (OMICRON). Silicon (111) samples (±0.5°) were resistively heated by a direct current. The surface cleaning procedure was carried out at pressures of $(1-2)\times10^{-10}$ Torr and consisted of a sample degassing for at least 4 h at 600 °C followed by flash at 1250 °C. The samples were cooled with the rate of about 50 °C min in the temperature range of 900–350 °C with a stepwise reduction of the heating current. Sr pieces encased in a Ta tube served as the source of Sr atoms. The Sr atoms were identified on silicon surface after deposition of extremely small amount (about 10^{-3} of a monolayer) of strontium on a sample at RT as noisy

areas in STM image, associated with fast Sr motion within the limits of Si(111)-7×7 HUC. All STM images were acquired at RT using an electrochemically etched tungsten tip. As it is common among experimentalists, we usually specify the sample bias so that the positive bias means that STM probes empty sample electronic states and vice versa.

The calculations reported here were performed by using the Siesta *ab initio* simulation package based on DFT with norm-conserving pseudopotentials and atomic orbitals as basis sets.[11] Pseudoatomic orbitals of Sankey-Niklewski type were used. The Sankey-Niklewski-type orbitals are the eigenfunctions of the (pseudo)atom within a spherical box (although the radius of the box may be different for each orbital). Core electrons were accounted for by using the pseudopotentials by Troullier and Martins.[12] The exchange-correlation functional is treated in the generalized gradient approximation (GGA).[13] It has been shown that for the description of surface adsorption, chemisorption, and particularly of saddle-point states, where bonds creation and annihilation take place, GGA appears to be superior to the local-density approximation (LDA).[14] The Brillouin-zone integration was carried out at the $\bar{\Gamma}$ point only. The use of single $\bar{\Gamma}$ point follows from the large lateral dimensions of the 7×7 unit cell. This approximation was used in a number of previous studies of the 7×7 reconstruction.[10,15] A uniform real-space grid equivalent to a plane-wave cutoff of 200 Ry has been used for numerical integration.

In order to make the problem computationally treatable, the following basis sets were used: SZ for H atoms (single-ζ $1s^1$), SZ for bulk Si atoms (single-ζ $3s^2 3p^2$; for two bottom Si bilayers), DZP for surface Si atoms (double-ζ $3s^2 3p^2$, single-ζ $3d^0$; for two upper Si bilayers and Si adatoms), and TZDP for Sr atom (triple-ζ $5s^2 5p^0 5d^0$). Following the nomenclature of quantum chemistry, a single-ζ (SZ) basis set has one single radial function per angular-momentum channel, double-ζ (DZ) basis set has two functions per angular-momentum channel, triple-ζ (TZ) has three, and so on. Angular flexibility is obtained by adding shells of higher angular momentum $l+1$ marked by P, where P stands for polarized, DP for double polarized, and so on. Thus, the numbers of basis functions per atom are: 1 for H, 4 for Si bulk atoms, 13 for Si surface atoms, and 27 for the Sr atom. Test calculations using a DZP basis set for Sr atom (double-ζ $5s^2$, single-ζ $5p^0$; five basis functions) were also performed, but the descriptions of the surface chemistry when comparing to the TZDP results were found unsatisfactory. Test calculations including Sr semicore states using a SZ-semicore DZP basis set (single-ζ $4s^2 4p^2 4d^0$ double-ζ $5s^2$ single-ζ $5p^0$; 14 basis functions per Sr atom) were also performed. These results are found to be almost identical to those obtained using TZDP basis set (see the discussion below). The latter test indicates that Sr semicore states do not participate in surface bonding chemistry (at least to a significant degree). Hence, Sr semicore states are hereafter accounted by the pseudopotential and a TZDP basis set is employed to represent Sr valency.

The supercell geometry used in this study consists on a repeating slab of four atomic Si bilayers and a vacuum region of 11 Å. The same slab thickness was used in previous studies of Pb and Si adsorption on Si(111)-7×7 surface.[9,10] The calculated band structure of the clean Si(111)-7×7 surface shows good agreement with that reported earlier by Bechstedt *et al.* in Ref. 16 where eight bilayer slabs were used. We, therefore, do not expect any significant changes if the calculations were repeated on slabs thicker than four bilayers.

The 7×7 dimer-adatom-stacking-fault (DAS) model of Takayanagi *et al.*[17] is used to fulfill the periodic boundary conditions along the lateral directions. The adsorbed Sr atom is added to the reconstructed 7×7 surface and the dangling bonds at the unreconstructed bottom surface are saturated by hydrogen atoms making 1.5 Å Si-H bonds. There are a total of 446 atoms in the supercell. In all calculations, the top three atomic Si bilayers are fully relaxed and the bottom Si bilayer with hydrogen atoms are kept at the bulk positions. The lattice constant a and the Kohn-Sham energy gap E_g for a bulk calculation (GGA and DZP basis) are 5.490 Å and 0.68 eV, respectively.

We carried out a thorough map of the PES describing the Sr atom on top of the Si(111)-7×7 surface. Accordingly, the Sr atom is initially placed 3 Å above the surface (this height is measured from the level of the Si adatoms) and its height (along the Z direction) is allowed to relax, while coordinates in the XY plane are kept fixed. The geometry is optimized until the atomic forces become less than 0.04 eV/Å. The calculations are performed for positions of the adsorbed Sr atom inside a symmetry-irreducible region of the surface unit cell which is only 1/6th of the area of the 7×7 unit cell.[10] A total of 190 points forming a hexagonal lattice with 0.86 Å spacing were initially calculated in the symmetry-irreducible wedge. Starting from the positions of energy minima and main diffusion paths, 29 additional points were calculated in these areas (0.43 Å lattice spacing). The complete PES for 7×7 unit cell was retrieved applying a C_{3v} symmetric transformation to the irreducible PES wedge data.

III. RESULTS AND DISCUSSION

A. Potential energy surface

Figure 1(a) shows the calculated PES for the adsorption of a Sr atom on the Si(111)-7×7 surface. In this figure, the faulted 7×7 HUC is overlaid with the DAS model of Takayanagi *et al.*[17] According to the DAS model, the Si dangling bonds are located at the rest atoms, adatoms, and corner hole atom. The energy of the most stable state in Fig. 1 is set to 0.0 eV for reference. Bright (dark) regions in the figure indicate minima (maxima) and, hence, they refer to favorable adsorption positions (unstable and saddle-point configurations). From this figure, we can immediately identify the most stable adsorption sites inside of 7×7 HUCs and migration paths between them. The most stable adsorption sites or basins of attraction are located around rest atoms [1→2→1 path in Fig. 1(a)]. Each HUC contains three such basins and they are connected by 3→4→5 type paths. Point 4 is a saddle point and it is located at the HUC center. Basins located at neighboring HUCs are connected by 3→6→7 type paths. These are "camel back" potential paths, where the metastable midpoint stands between two adjacent Si dimers

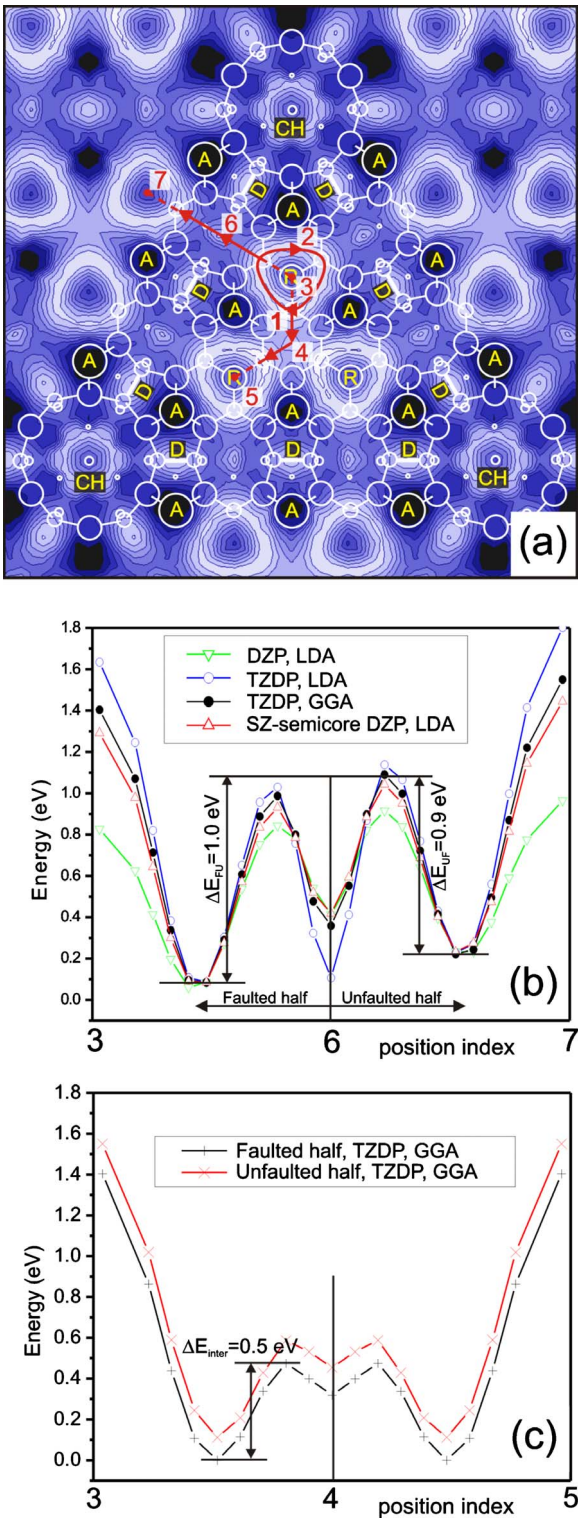

FIG. 1. (Color online) (a) PES for the adsorption of Sr atom on the Si(111)-7×7 surface. The faulted 7×7 HUC with overlaid DAS model of Takayanagi *et al.* (Ref. 17) is shown. Larger symbol indicate topmost atoms. A—Si adatom, D—dimer, R—rest atom, CH—corner hole. The contour spacing is 0.2 eV. Bright (dark) regions indicate energy minima (maxima) and, hence, favorable adsorption positions (transition-state regions). Solid arrows show the main migration paths for Sr atom. [(b) and (c)] The profiles of PES along (b) 3→6→7 and (c) 3→4→5-type paths indicated by solid arrows and dashed lines in (a).

in the HUC edge. Note that although adatom, rest atom, and corner hole atom positions possess reactive Si dangling bonds, they exhibit local or global energy maxima. Adsorption instability at these sites may follow from the twofold valency of Sr, suggesting that monocoodinated Sr is highly unstable. Paths of type 1→2→1, 3→4→5, and 3→6→7 form a network, which spans the entire Si(111)-7×7 surface. The energy barriers found in these paths determine Sr dynamics on this surface. The most stable adsorption sites for Sr are the same as those found for adsorption of K, Mg, Ga, Ge, Si, and Pb on the Si(111)-7×7 surface.[7,9]

Figure 1(b) shows the PES profile along a 3→6→7-type path in Fig. 1(a) calculated using different approximations for the exchange-correlation energy (LDA or GGA) and different basis sets for the Sr adatom (DZP or TZDP), including with and without Sr semicore $4s^2 4p^2 4d^0$ states. The graph shows that all four profiles calculated using different parameters are in qualitative agreement. It shows a deep energy minimum between Si dimers in the HUC edge, although the energy barriers may differ depending on the calculation conditions. For the "DZP, LDA" calculation, the energy barrier for Sr jump from faulted to unfaulted (FU) HUC is ΔE_{FU} =0.8 eV (ΔE_{UF}=0.7 eV from unfaulted to faulted HUC), while it is ΔE_{FU}=1.0 eV (ΔE_{UF}=0.9 eV) for "TZDP, LDA" and "TZDP, GGA" calculations. The stronger corrugation of PES at TZDP basis set for Sr atom indicates the lack of variational freedom in DZP basis and an inaccurate calculation in this case. The difference between TZDP, LDA and TZDP, GGA profiles is much smaller, so that all relevant energy barriers are consistent within 0.1 eV. The energy profiles calculated using TZDP, GGA and "SZ-semicore DZP, LDA" are almost undistinguishable.

Figure 1(c) shows the PES profile along the 3→4→5-type path in Fig. 1(a) calculated using TZDP basis set for Sr atoms and GGA for exchange-correlation energy. The profile shows a shallow depression at the middle of the path, i.e., at the center of the HUC. The energy barrier for such interbasin jump (jump between basins within the same HUC) is found to be $\Delta E_{\mathrm{inter}}$=0.5 eV for both faulted and unfaulted HUCs. The energy difference between sites 1 and 2 located *in* the same basin is only $\Delta E_{\mathrm{intra}}$=0.1 eV for both faulted and unfaulted HUCs, so that site 1 is slightly more favorable than site 2. The preference for sites located closer to the HUC center over sites located closer to the HUC corners was first found for Si (Ref. 10) and then for Pb (Ref. 9) atoms. According to our calculation, the energy increases from site 1 to site 2 smoothly.

Apparently, the low-energy barrier along 1→2→1 path is due to high concentration of Si dangling bonds in this area. When moving along this path, a Sr-Si bond is established with a Si rest atom and a second bond is made with a Si adatom. During such orbital motion, although the Sr–rest atom bond is always preserved, the second bond switches from one Si adatom to another. Since Si adatoms in the 7×7 DAS reconstruction are located close to each other, bond breaking and creation happens concurrently and this leads to a low-energy barrier. The motion along 3→4 or 3→6-type paths involves breaking a Sr–rest atom bond and this leads to the high-energy barriers found in these paths.

The hopping rates along different paths at RT can be estimated assuming a thermally activated motion. Accordingly,

the jump rate is $\nu = \nu_0 \exp(-\Delta E/k_B T)$, where ΔE is the barrier height, k_B is the Boltzmann constant, T is the temperature, and ν_0 is a characteristic phonon frequency of the system.[18] The latter can be taken equal to the Debye frequency for Si: $\nu_0 = 14$ THz. Thus, we get $\nu_{FU} = 2.4 \times 10^{-4}$ Hz (characteristic time $t_{FU} = 1/\nu_{FU} = 4200$ s), $\nu_{UF} = 1.1 \times 10^{-2}$ Hz ($t_{UF} = 90$ s), and $\nu_{inter} = 57.8$ MHz ($t_{inter} = 1.73 \times 10^{-5}$ s). The equation is not applicable for Sr movement inside the basin, since the energy barrier $\Delta E_{intra} = 0.1$ eV is comparable to $k_B T = 0.03$ eV at RT. For such a small energy barrier, at RT, the Sr atom can move almost freely around the rest atoms along the path $1 \rightarrow 2 \rightarrow 1$. It should be noted that the actual hopping rates for $3 \rightarrow 4 \rightarrow 5$ and $3 \rightarrow 6 \rightarrow 7$ type paths should be at least a factor $k \approx 100-1000$ smaller than the calculated values due to configurational degeneracy.[19] Even for such a reduction of the hopping rates, taking the scan rate of a typical STM system to be 10^{-2} Hz ($t = 100$ s), we still can conclude that Sr atoms visit all basins within a given HUC many times during the acquisition period of a single STM image. Conversely, Sr hops between HUCs are much rarer. This indeed agrees with the experimental observations.[3]

The migration paths for Sr in unfaulted HUC are found to be the same as in faulted HUC, albeit energies in unfaulted HUC sites are about 0.1 eV higher than analogous energies in faulted HUCs. Thus, the Sr atom should preferentially occupy faulted HUCs. According to the principle of detailed balance,[18] the number of Sr atoms located in unfaulted (N_U) and faulted (N_F) HUCs should relate as $N_U/N_F = \exp(-\Delta E/k_B T) = 0.02$ in equilibrium at RT. Therefore, under thermodynamic equilibrium, only about 2% of the Sr atoms will be located at unfaulted HUCs, while the majority of them will be found at faulted HUCs. The preferential adsorption of adatoms at faulted HUCs of the Si(111)-7×7 for low coverages has been reported for a variety of metals, such as Pb, Tl, Sn, Ag, Pd,[20] and the alkali metals.[21] Our results suggest that this is also the case for Sr.

B. Scanning tunneling microscopy images

Figure 2 shows a set of empty and filled states STM images of single Sr atoms confined within a 7×7 HUC obtained at RT. The Sr atom manifests itself in the image as an apparently noisy patch with streaks along the X direction. The shape of the image streaks, elongated in X direction, is related to the movement of the tip which scans the image line by line with the X axis being the fast scanning direction. We have shown recently that the length of such streaks depends on the scanning tip velocity and therefore it allows the speed of the captured adatom to be deduced.[3]

According to a simplistic picture, one would interpret the higher density of image streaks (or higher brightness in STM images) as a higher relative residence time of the adsorbed atom. Since this atom should move along low-energy diffusion paths at the PES, the experimental STM images should resemble the bright shapes of the PES in Fig. 1(a). This is, however, definitely not the case.

One possible issue is that the tip may be too coarse to resolve the fine features form the PES pattern. As shown previously, at least 0.3 nm widening of image features should be assumed.[3] Another possible issue is that an influence of the scanning tip on the movement of the Sr atom cannot be completely excluded. Still, these issues cannot satisfactorily explain the striking difference between PES and STM images. Most importantly is that both topography and electronic states influence the brightness in STM images and these contributions cannot be easily separated. The strong bias dependence of the STM images in Fig. 2 indicates that the image contrast is mostly electronic in origin and not a topographic feature. This implies that the brightness of the experimental image features in the 7×7 HUC cannot be simply interpreted as relative residence time of a moving Sr atom. This would be justified only when studying a moving atom on an unreconstructed surface with uniform chemical composition, for example, on flat metallic surfaces.

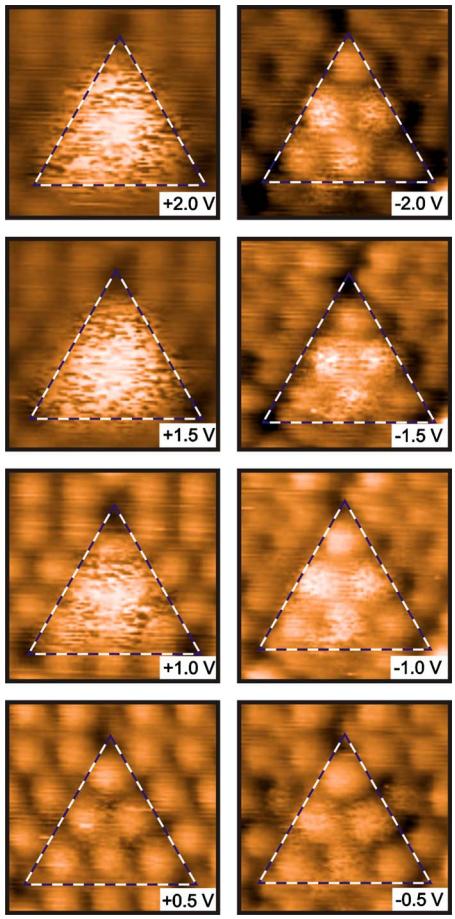

FIG. 2. (Color online) Empty (left) and filled (right) states experimental STM images of a moving Sr atom within the limits of the 7×7 HUC, taken with sample bias ±0.5, ±1.0, ±1.5, and ±2.0 V at RT. The 7×7 HUC with trapped Sr atom is outlined by dashed line. Scan speed is 50.0 nm/s.

Several STM image features in Fig. 2 should be highlighted. First, the streaks associated with the Sr movement are brighter in empty states images than in filled states. Second, at high bias ($U = \pm 1.0, \pm 1.5, \pm 2.0$ V) image streaks are visible, while they almost vanish at low bias ($U = \pm 0.5$ V). A similar experimental observation was carried out for an Al atom captured within a Si(111)-7×7 HUC.[4]

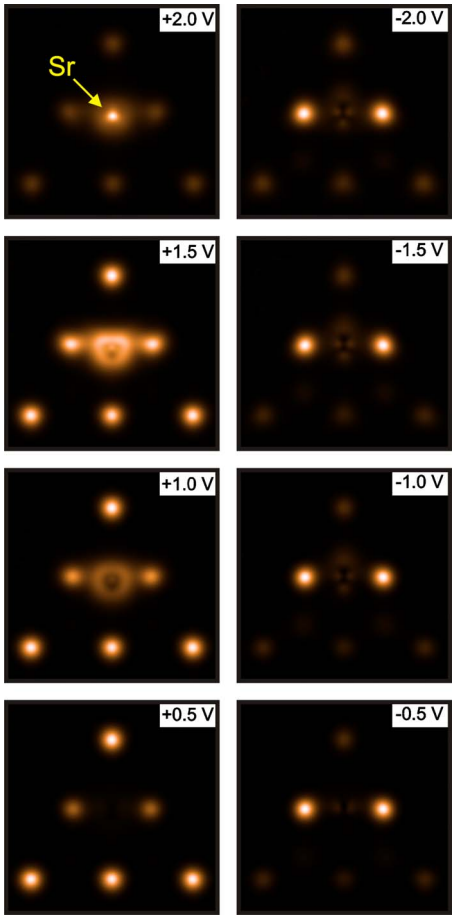

FIG. 3. (Color online) Simulated STM images of empty (left panel) and filled (right panel) states of the Sr atom located in site 1 of the faulted 7×7 HUC [see Fig. 1(a)] for bias voltages corresponding to ±0.5, ±1.0, ±1.5, and ±2.0 eV with respect to the theoretical Fermi level.

Third, the Si adatoms are brighter for the 7×7 HUC with a Sr atom than empty 7×7 HUC (in filled states STM images). Moreover, the three center Si adatoms appear in these images brighter than adatoms located close to corner holes. Below, we present the results of our simulations of these STM image features and discuss their origin.

Figure 3 shows a set of empty and filled states simulated STM images of faulted 7×7 HUC with a Sr adatom located in site 1 of Fig. 1(a). These simulations were carried out according to the Tersoff-Hamann approximation[22] at constant-height mode. It represents the local density of states integrated between the Fermi level and the level corresponding to the applied voltage at certain height above the surface. The Si adatoms exhibit themselves as bright spots at the apexes and midsides of equilateral triangles. One can see that our simulation correctly reproduces the voltage dependence of experimental STM images: although being less visible in negative bias images, the Sr atom is visible at $U=\pm1.0, \pm1.5, \pm2.0$ V, but not detected at $U=\pm0.5$ V. This suggests that the Sr adatom is electrically inert and Sr-related bonding and antibonding states lie within the valence and conduction bands of Si. Unfortunately, it is difficult to visualize these states because they mix with the crystalline host states.

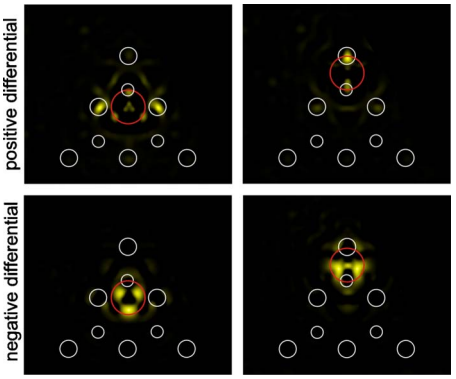

FIG. 4. (Color online) Gray scale image showing the positive and negative differentials of the charge density of a Sr atom at 1 (left panel) and 2 (right panel) bonding sites in Fig. 1(a) with respect to the reference charge density. Circles in the figure indicate the positions of the Sr atom (the largest circle), Si adatoms (medium circles), and Si rest atoms (smallest circles).

One can also see in Fig. 3 that the Sr atom is much better visible in empty states simulated STM images than in filled states. Note also that the Si adatoms neighboring the Sr atom changed their voltage polarity dependence: they appear darker in empty state images and brighter in filled state ones. In other words, the empty states are localized mainly on the Sr atom, while the filled states are on Si adatoms neighboring the Sr atom. This result shows that a charge transfer from the Sr atom to the closest Si adatoms takes place.

The Mulliken population analysis shows that the charge transferred from the Sr atom to the surface is $0.25e$ $(0.22e)$ when the Sr atom is located at site 1 (site 2) of the 7×7 HUC shown in Fig. 1(a). There is also a large redistribution of the charge in the surroundings of the Sr atom. According to the Mulliken charges, the shape of the charge-density distribution around the Sr atom is changed considerably when compared to isolated Sr atom, where both valence electrons are on the $5s$ orbital. Accordingly, only 0.48 (0.47) electrons are found on the $5s$ orbital when the Sr atom is located at site 1 (site 2), while the remaining electrons are found on the $5p$ orbital 0.56 (0.63) and $5d$ orbital 0.71 (0.69), respectively.

The charge-density redistribution due to interaction between Sr adatom and Si(111)-7×7 substrate is further analyzed in Fig. 4. This figure is obtained by subtracting from the system charge density, $n_{\mathrm{Sr/Si(111)\text{-}7\times7}}(x,y,z)$, a reference charge density.[23] The latter is constructed by adding the densities of an isolated Sr atom $n_{\mathrm{Sr}}(x,y,z)$ and the free substrate $n_{\mathrm{Si(111)\text{-}7\times7}}(x,y,z)$ (with positions fixed at the final-relaxed location) for sites 1 and 2, respectively. Thus, the reference charge density represents the charge density of noninteracting Sr adatom and Si(111)-7×7 substrate. The resulting three-dimensional (3D) charge-density difference was integrated along Z direction

$$\Delta n(x,y) = \int [n_{\mathrm{Sr/Si(111)\text{-}7\times7}} - n_{\mathrm{Sr}} - n_{\mathrm{Si(111)\text{-}7\times7}}]dz$$

and is plotted in Fig. 4. The negative and positive differentials of the projected charge density are shown separately.

The integrated intensity in the figure gives the total amount of the charge that is redistributed upon the formation of the bonds, which amounts to 0.65 (0.74) electrons for site 1 (site 2). Charge-density depletion areas are localized around the Sr atom. The charge is redistributed to the surface atoms, most strongly to the closest Si adatoms and Si-rest atom. This is in contrast to directional covalent bonding where the buildup of charge should be observed in the zone between the Si dangling bond and the adsorbed atom. This indicates that although the bonding between Sr atom and the surface still has a predominant covalent character (the total charge redistribution is much larger than the charge transfer obtained by the Mulliken analysis), it demonstrates also some ionic character, which is more pronounced than in case of Ba adsorption on Si(100).[23] This is also confirmed by higher values of the Mulliken charge obtained for Sr on Si(111) (+0.25*e* for site 1 and +0.22*e* for site 2) than for Ba on Si(100) (+0.15*e*). The charge redistribution analysis also indicates a small charge transfer from the Sr atom to Si adatoms in unfaulted HUC, i.e., to regions quite distant from the Sr atom. It should be noted that the charge transferred from the Sr atom to the Si rest atoms has a small impact on the STM images. This is because their height level is ~1 Å below the level of Si adatoms.

Figure 5 shows the calculated Kohn-Sham electronic band structures of clean (a) and Sr adsorbed (b) Si(111)-7×7 slab surfaces along the highly symmetric $\bar{\Gamma}$-$\bar{M}_{7\times7}$ direction. From inspection of the squared Kohn-Sham states at $\bar{\Gamma}$, we found that the states with energies lying within the fundamental energy gap are mainly localized on Si adatoms, while states edging the valence band are mainly localized on rest and corner hole atoms. Thus, the bonds localized on rest atoms and corner hole atom are fully saturated, while the bonds localized on adatoms are partially depopulated due to charge transfer from Si adatoms to rest atoms and corner hole atom on a clean Si(111)-7×7 surface. This result agrees with a previous study of Si(111)-7×7 by Stekolnikov *et al.*[24] One can note in Fig. 5(b) that upon Sr adsorption, several band lines associated with Si adatoms shifted downwards in energy. Those lines which shift most significantly are marked by arrows in Fig. 5(a). This indicates higher occupancy of surface states localized on Si adatoms when Sr is adsorbed. Again, this the consequence of charge transfer from Sr atom to neighboring Si adatoms.

The flat energy path 1-2-1 is surrounded by three equivalent Si adatoms. The brightness of Si adatoms in filled states STM images switches between the three combinations of adatom pairs during the orbital motion of the Sr atom around the rest atom as shown in Fig. 6. This figure is particularly insightful as it explains why three Si adatoms located at the HUC center appear brighter than three adatoms close to the corner hole in experimental filled states STM images. The first reason is that according to the PES presented in Fig. 1(a), the Sr atom has a slight preference to sit at site 1 than at site 2. The second reason is geometrical: while each center adatom has two neighboring rest atoms, the adatom located close to the corner hole has only one. Thus, considering the orbiting Sr atom around each rest atom, we find that it can be found twice more often close to center adatoms than to corner adatoms. This idea is schematically illustrated in Fig. 7.

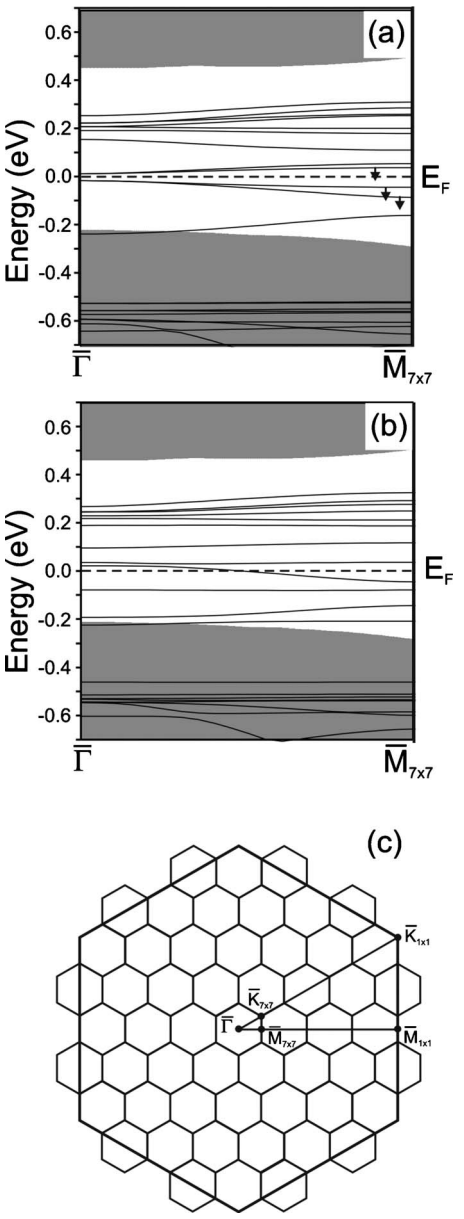

FIG. 5. [(a) and (b)] Surface band structures along the highly symmetric $\bar{\Gamma}-\bar{M}_{7\times7}$ direction in the corresponding two-dimensional (2D) Brillouin zone of 7×7 reconstruction. The projected bulk band structures around the fundamental gap are presented as shaded areas. (a) Band structure of clean 7×7 reconstruction. (b) Band structure of 7×7 reconstruction with Sr atom adsorbed in site 1 of Fig. 1(a). The states whose band lines are within the fundamental gap are localized on Si adatoms while whose band lines are in valence band are localized on rest and corner hole atoms. Arrows in (a) indicate band lines which shift downwards most considerably upon Sr adsorption. (c) Schemes of 2D Brillouin zones for 1×1 and 7×7 cells.

Summing up the above findings, one can say that at positive bias, STM is more sensitive to the Sr atom, while at negative bias, the Si adatoms in the 7×7 reconstruction are more prominently revealed. Still, this does not mean that the brightness in STM images at positive bias correctly reflects

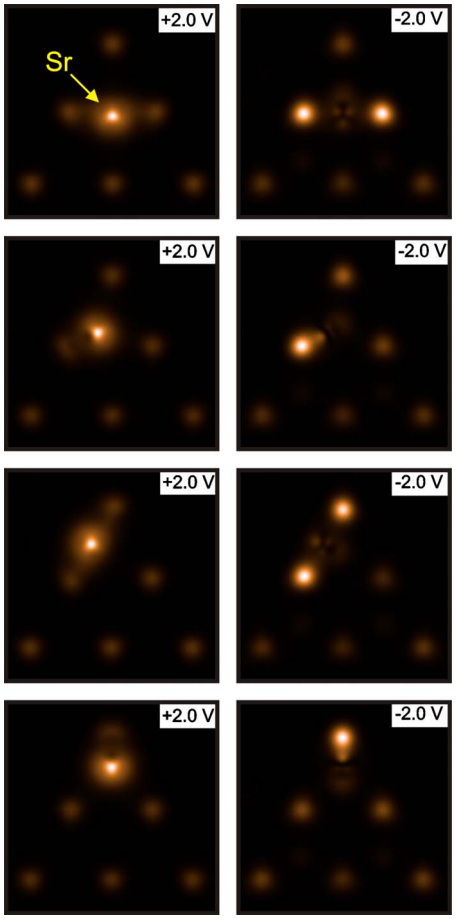

FIG. 6. (Color online) Simulated STM images of empty (left) and filled (right) states of the Sr atom located in four different sites along the $1 \rightarrow 2$ path for bias voltages corresponding to ± 2.0 eV with respect to the theoretical Fermi level. Upper panel: site 1 in Fig. 1(a); lower panel: site 2 in Fig. 1(a); two panels in the middle: intermediate positions.

the relative residence time of Sr atom. This follows from the low probability of finding the Sr atom at energy maxima (on top of Si adatoms for example), which is partially compensated by the closer position to STM tip due to elevated height.

The explanation of the intensity distribution in STM images based on charge transfer from the Sr atom to neighboring Si adatoms of the 7×7 reconstruction should be valid for a number of other chemical species. For example, Sato *et al.* reported STM images similar to Fig. 2 when a Si atom was trapped at the HUC of a 7×7 reconstruction (see Fig. 5 of Ref. 5). The authors interpreted the brightness in those STM images as the relative residence time (or "rate of residence" as they refer) of a diffusing Si atom. Again, as in the case of Sr, one can see the striking difference between the STM images in Fig. 5 of Ref. 5 and the PES image for a Si atom on Si(111)-7×7 HUC in Fig. 1 of Ref. 10. Similar to the Sr case, the intensity distribution in STM images in the Si case is strongly influenced by electron transfer from the attacking Si atom to Si adatoms in the 7×7 DAS reconstruction. The charge transfer is possible because these atoms are chemically distinct. This was directly checked in our simulations.

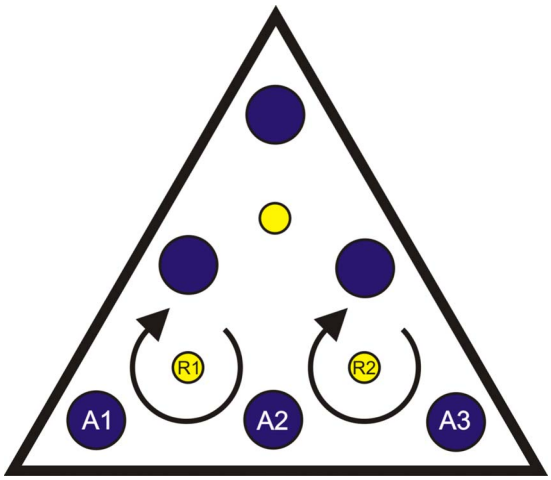

FIG. 7. (Color online) Schematic illustrating the idea that Sr atom can be found twice more often close to center adatoms (A2) than to corner adatoms (A1, A3) when considering the orbiting Sr atom around each rest atom (R1, R2) consequently.

The Sr atom at site 1 shown in Fig. 1(a), which is the most stable site for a Si atom as well, was replaced by Si and empty and filled states STM images were simulated. The effect of a similar charge transfer was clearly visible in these images, although it was less pronounced than in the case of Sr. This implies that the former interpretation of brightness in STM images of the apparently noisy patches as the relative residence time of a diffusing Si atom is at least partially incorrect. An explanation complemented by a charge-transfer effect is needed to account for the observations.

The simulation results reported here are in complete agreement with a local chemical reactivity analysis using electronegativity and local softness concepts as suggested by Brommer *et al.*[25] Sr electronegativity of 2.0 eV was taken from Pearson's estimation.[26] The surface electronegativity is the work function, 4.8 eV. Since the difference in electronegativity between the surface and the Sr atom is positive, then Sr is the electron donor. Each Si adatom close to the HUC center in the 7×7 reconstruction has two neighboring rest atoms, while the corner adatom has only one. This explains the higher depopulation rate of dangling bonds located on adatoms close to the HUC center relative to bonds on corner adatoms due to charge transfer to rest atom dangling bonds. Since the bonding between the Sr atom and the Si(111)-7×7 surface is partially ionic in origin, i.e., it follows from a charge-transfer process, then the strongest Sr interaction should occur with Si adatoms at the HUC center and a little bit weaker with corner adatoms.[25] This correlates with a weak preference of site 1 over site 2 in Fig. 1(a) for Sr adsorption.

IV. CONCLUSION

Sr adsorption and diffusion on Si(111)-7×7 are investigated both experimentally using STM and theoretically via mapping of the potential-energy surface using DFT calculations. The deepest minima or basins of attraction are found around rest atoms in both faulted and unfaulted HUCs in

accordance to previous studies for other adsorbates. The main diffusion path between basins of the same HUC is through the HUC center. The corresponding energy barrier is 0.5 eV. Sr migration between basins located at neighboring HUCs takes place between Si dimers in the HUC edge. The corresponding energy barriers are 1.0 eV for hopping from faulted to unfaulted HUC and 0.9 eV vice versa.

Simulated STM images and one-electron band structures for the Sr atom adsorbed on the Si(111)-7×7 surface are reported. The simulated STM images correctly reproduce voltage and polarity dependence of the experimental observations. It was found that the peculiar distribution of the intensity in STM images is due to electron transfer from the Sr atom to Si adatoms in the 7×7 reconstruction. As a result, at positive bias, STM is more sensitive to the Sr atom, while at negative bias, the Si adatoms are more prominent. The proposed explanation for observed intensity distribution solves the contradiction between the experimental STM imagery of Si(111)-7×7 HUCs with captured adatoms and calculated potential-energy surfaces reported in the literature.

ACKNOWLEDGMENTS

We thank the Novosibirsk State University for providing us with computational resources. We acknowledge financial support by FCT Portugal (Grant No. SFRH/BPD/38291/2007) and by Russian Foundation for Basic Research (Grants No. 10-02-00199 and No. 08-02-01101).

[1] R. A. McKee, F. J. Walker, and M. F. Chisholm, Phys. Rev. Lett. **81**, 3014 (1998).
[2] S. Teys, B. Olshanetsky, R. Zhachuk, S. Pereira, and G. Norga, Appl. Phys. Lett. **93**, 161912 (2008).
[3] R. Zhachuk, S. Teys, B. Olshanetsky, and S. Pereira, Appl. Phys. Lett. **95**, 061901 (2009).
[4] H. Uchida, T. Kuroda, F. B. Mohamad, J. Kim, K. Kashiwagi, K. Nishimura, and M. Inoue, Phys. Status Solidi B **241**, 1665 (2004).
[5] T. Sato, S. Kitamura, and M. Iwatsuki, Surf. Sci. **445**, 130 (2000).
[6] J. M. Gómez-Rodríguez, J. J. Sáenz, A. M. Baró, J.-Y. Veuillen, and R. C. Cinti, Phys. Rev. Lett. **76**, 799 (1996); L. Vitali, M. G. Ramsey, and F. P. Netzer, *ibid.* **83**, 316 (1999); H. Uchida, S. Watanabe, H. Kuramochi, J. Kim, K. Nishimura, M. Inoue, and M. Aono, Phys. Rev. B **66**, 161316(R) (2002); J. Mysliveček, P. Sobotík, I. Ošt'ádal, T. Jarolímek, and P. Šmilauer, *ibid.* **63**, 045403 (2001); C. Polop, E. Vasco, J. A. Martín-Gago, and J. L. Sacedón, *ibid.* **66**, 085324 (2002); H. Uchida, S. Watanabe, H. Kuramochi, M. Kishida, J. Kim, K. Nishimura, M. Inoue, and M. Aono, Surf. Sci. **532-535**, 737 (2003); O. Custance, I. Brihuega, J. M. Gómez-Rodríguez, and A. M. Baró, *ibid.* **482-485**, 1406 (2001).
[7] K. Cho and E. Kaxiras, Surf. Sci. **396**, L261 (1998).
[8] R. L. Lo, I. S. Hwang, M. S. Ho, and T. T. Tsong, Phys. Rev. Lett. **80**, 5584 (1998); A. Vittadini and A. Selloni, *ibid.* **75**, 4756 (1995); R. L. Lo, M. S. Ho, I. S. Hwang, and T. T. Tsong, Phys. Rev. B **58**, 9867 (1998); H. Lim, K. Cho, I. Park, J. D. Joannopoulos, and E. Kaxiras, *ibid.* **52**, 17231 (1995).
[9] O. Custance, S. Brochard, I. Brihuega, E. Artacho, J. M. Soler, A. M. Baró, and J. M. Gómez-Rodríguez, Phys. Rev. B **67**, 235410 (2003).
[10] C. M. Chang and C. M. Wei, Phys. Rev. B **67**, 033309 (2003).
[11] J. M. Soler, E. Artacho, J. D. Gale, A. Garcia, J. Junquera, P. Ordejón, and D. Sánchez-Portal, J. Phys.: Condens. Matter **14**, 2745 (2002); http://www.icmab.es
[12] N. Troullier and J. L. Martins, Phys. Rev. B **43**, 1993 (1991).
[13] J. P. Perdew, K. Burke, and M. Ernzerhof, Phys. Rev. Lett. **77**, 3865 (1996).
[14] B. Hammer, M. Scheffler, K. W. Jacobsen, and J. K. Norskov, Phys. Rev. Lett. **73**, 1400 (1994).
[15] K. D. Brommer, M. Needels, B. E. Larson, and J. D. Joannopoulos, Phys. Rev. Lett. **68**, 1355 (1992); I. Štich, M. C. Payne, R. D. King-Smith, J-S. Lin, and L. J. Clarke, *ibid.* **68**, 1351 (1992).
[16] F. Bechstedt, A. A. Stekolnikov, J. Furthmüller, and P. Käckell, Phys. Rev. Lett. **87**, 016103 (2001).
[17] K. Takayanagi, Y. Tanishiro, and M. Takahashi, Surf. Sci. **164**, 367 (1985).
[18] F. Bechstedt, *Principles of Surface Physics* (Springer, Berlin, 2003).
[19] An estimate of the reduction of the hopping rate k due to configurational degeneracy can be done in following way. The Sr atom can jump to another basin only if it is located in front of corresponding path. Since the energy difference between 1 and 2 sites is small (ΔE_{intra}=0.1 eV), we can assume for simplicity that at room temperature, the Sr atom can be found at any location along the basin with equal probability. Hence, the fraction of time that the Sr atom spends in front of the corresponding path is $k=W/L$, where W stands for the width of corresponding migration path and L is length of basin loop.
[20] St. Tosch and H. Neddermeyer, Phys. Rev. Lett. **61**, 349 (1988); U. K. Kohler, J. E. Demuth, and R. J. Hamers, *ibid.* **60**, 2499 (1988); E. Ganz, F. Xiong, I.-S. Hwang, and J. Golovchenko, Phys. Rev. B **43**, 7316 (1991); D. Tang, H. E. Elsayed-Ali, J. Wendelken, and J. Xu, *ibid.* **52**, 1481 (1995); X. F. Lin, I. Chizhov, H. A. Mai, and R. F. Willis, Surf. Sci. **366**, 51 (1996).
[21] T. Hashizume, K. Motai, Y. Hasegawa, I. Sumita, H. Tanaka, S. Amano, S. Hyodo, and T. Sakurai, J. Vac. Sci. Technol. B **9**, 745 (1991); A. Watanabe, M. Naitoh, and S. Nishigaki, Jpn. J. Appl. Phys. **37**, 3778 (1998).
[22] J. Tersoff and D. R. Hamann, Phys. Rev. Lett. **50**, 1998 (1983); Phys. Rev. B **31**, 805 (1985).
[23] J. Wang, J. A. Hallmark, D. S. Marshall, W. J. Ooms, P. Ordejón, J. Junquera, D. Sánchez-Portal, E. Artacho, and J. M. Soler, Phys. Rev. B **60**, 4968 (1999).
[24] A. A. Stekolnikov, J. Furthmüller, and F. Bechstedt, Phys. Rev. B **65**, 115318 (2002).
[25] K. D. Brommer, M. Galván, A. Dal Pino, and J. D. Joannopoulos, Surf. Sci. **314**, 57 (1994).
[26] R. G. Pearson, Inorg. Chem. **27**, 734 (1988).